ESD-TR-90-112

Technical Report
903

Design of a Small-Aperture Steering Mirror for High-Bandwidth Acquisition and Tracking

G.C. Loney

26 October 1990

Lincoln Laboratory

MASSACHUSETTS INSTITUTE OF TECHNOLOGY

LEXINGTON, MASSACHUSETTS

**Prepared for the Department of the Air Force
under Contract F19628-90-C-0002.**

This report is based on studies performed at Lincoln Laboratory, a center for research operated by Massachusetts Institute of Technology. The work was sponsored by the Department of the Air Force under Contract F19628-90-C-0002.

This technical report has been reviewed and is approved for publication.

FOR THE COMMANDER

Hugh L. Southall

Hugh L. Southall, Lt. Col., USAF
Chief, ESD Lincoln Laboratory Project Office

MASSACHUSETTS INSTITUTE OF TECHNOLOGY
LINCOLN LABORATORY

DESIGN OF A SMALL-APERTURE STEERING MIRROR FOR HIGH-BANDWIDTH ACQUISITION AND TRACKING

G.C. LONEY
Group 71

TECHNICAL REPORT 903

26 OCTOBER 1990

LEXINGTON MASSACHUSETTS

ABSTRACT

The High-Bandwidth Steering Mirror (HBSM) prototype is the product of a research program to develop a high-bandwidth, low angular range, two-dimensional beam steerer used in optomechanical pointing, acquisition, and tracking systems. This research centered around the optimization of a beam-steering mechanism comprising a mirror, restoring flexure, actuators, position sensors, and encompassing housing. Various design trade-offs and manufacturing issues involved in building the prototype are discussed, and the resulting performance data are presented. The resulting HBSM design allows integration with a simple closed-loop control scheme. The mirror/controller has a closed-loop bandwidth of 10 kHz, and 1° peak-to-peak stroke (mirror normal) at low frequencies. This increased bandwidth yields excellent disturbance rejection in the 10- to 1000-Hz frequency band and enables the generation of faster scan patterns.

ACKNOWLEDGMENTS

I would like to acknowledge Eric Swanson and Dr. James Roberge for their contributions to this work. I would also like to thank the Innovative Research Program at Lincoln Laboratory for sponsoring this research.

TABLE OF CONTENTS

LIST OF ILLUSTRATIONS

LIST OF TABLES

1. INTRODUCTION

The device described in this report, the High-Bandwidth Steering Mirror (HBSM), functions under high-bandwidth feedback control to point a 16-mm aperture mirror in two dimensions.

The HBSM can be used in a number of optomechanical systems where pointing, tracking, or acquistion is performed. Similar devices have been used to stabilize a space-based or airborne optical system's line-of-sight (LOS) [1] in the presence of external disturbances or jitter. This jitter is usually broadband in nature, from DC to 1 kHz. Previous mirror systems [2,3] have been very successful in rejecting this disturbance spectrum up to 100 Hz, but as optical systems are pushed to greater pointing accuracies (hundreds of nanoradians), rejection in the 100-Hz to 1-kHz band becomes important. The peak-to-peak angular stroke (shaft space) required in this operation is on the order of one milliradian. In an alternate mode, where the mirror may be commanded to scan some field of view or acquire a target, the angular stroke required is on the order of one to several degrees.

A small research program was initiated to investigate the design and buildup of these devices. Of particular interest were approaches to boosting the bandwidth performance of small-aperture steering mirrors to achieve greater disturbance rejection at high frequencies. It was also deemed desirable to use the mirror in a scan or acquisition mode. The primary goal of this program was to produce working hardware under closed-loop control with a 1° stroke and a 10-kHz, -3-dB point, closed-loop bandwidth. Consideration was given to making the device small, lightweight, and rugged.

The design process leading to the HBSM configuration, a description of the assembly, and relevant performance data are presented.

2. LOOP DESCRIPTION

The closed loop is made up of four major components: the mechanism (composed of a mirror blank, flexural support, and housing), actuators (to steer the mirror), sensors (to measure tilt), and compensation/drive electronics. All four components limit bandwidth, with some easier to correct for than others. These components are shown in Figure 1.

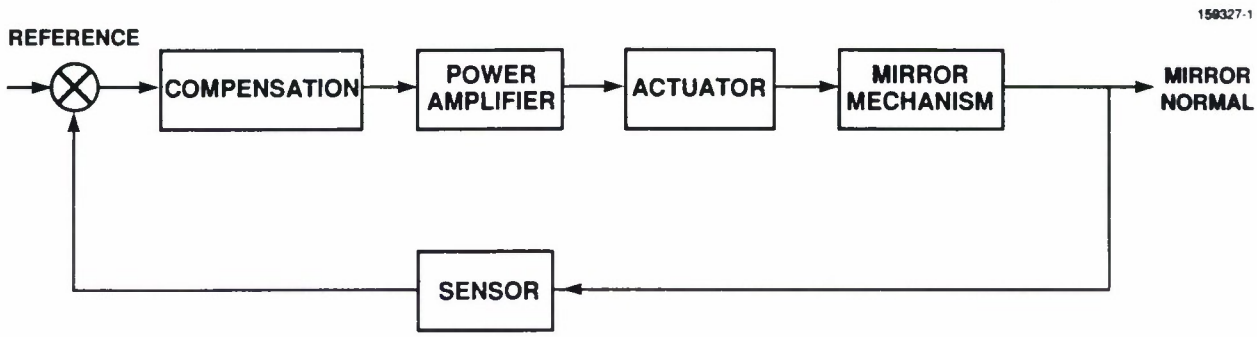

Figure 1. Fundamental blocks of the HBSM. The sensor block may represent a remote detector or sensors integral to the HBSM assembly.

Two common control-loop configurations are closed around the steering mirror. Each uses a different type of sensor: a track loop, in which the beam is nulled on a remote detector, causing the mirror to track the radiation source; and an acquisition loop, where integral sensors furnish the position feedback allowing the mirror to execute random moves or scan patterns.

Actuators and sensors limit high-bandwidth actuation through phase loss; these losses may be eliminated through electronic compensation. The drive electronics can be built with enough bandwidth (audio frequency band) so that performance is not severely impacted. In meeting the bandwidth goal, the actuators, sensors, and associated electronics are not seen to be severe limiters. The mechanism structure is the main limitation to high-bandwidth performance.

3. PLANT DYNAMICS

A simple steering-mirror mechanism is composed of a mirror mass (which must be attached to some actuator head/s), restoring spring or flexure mount, and housing. The optical system requirements drive the design of the mechanism: clear aperture sizes the mirror mass, angular stroke and required scan acceleration determine the type/size of the actuator, and volume and weight drive the housing design.

As a fairly large stroke was desired for the HBSM, an electromagnetic voice-coil actuator was chosen. When used with a properly designed current source, these actuators exhibit very high bandwidth but possess low peak force. This low peak force complicates the engineer's task in designing a high-bandwidth steering mirror. Thus, a "soft" system must be built to avoid overtaxing the actuators, but the system must also be "stiff" to achieve the desired fast response. Specifically, the transfer function between the mirror normal and actuator torque must exhibit certain behavior, which in practice is difficult to achieve. The response ideally would have a low-frequency resonance (set by the usable actuator torque, angular range, and moment of inertia of the mirror) representing the first rocking mode and no other significant modes coupling into rotation above that resonance. If this response can be obtained, it becomes a simple matter to close a stable loop by adding a lead network and proper gain. In reality, this classic second-order response is possible only in a select frequency band. If secondary modes do couple into rotation, the placement of stable, closed-loop poles in the complex plane may be difficult. The result is a system exhibiting undesirable oscillatory response or instability [4].

To better understand the mechanism dynamics, a simple two-degree-of-freedom rocking problem is studied. Figure 2 shows the key elements of such a problem: a rigid body representing a mirror mass m with rotational inertia J. connected to a vertical spring k_v, a lateral spring k_l, and a rotational spring k_r, holding the body in static equilibrium. The assumptions made in formulating the model are that the mass exhibits planar motion, that the vertical spring can be decoupled from the rocking and lateral motions, and that damping is small and neglected. These assumptions are not strictly correct; however, this simple model can yield useful insight into the parameter adjustment that might shape the mechanism frequency response.

The following expressions are useful in writing the coupled eigenvalue and eigenvector equations, with the uncoupled eigenvalues

$$\omega_r^2 = \frac{k_r}{J} \qquad \omega_l^2 = \frac{k_l}{m} \tag{1}$$

and the mass moment of inertia referenced to the base

$$J' = J + mh^2. \tag{2}$$

The parameters ω_r and ω_l are the natural frequencies of each uncoupled degree of freedom, rotation, and lateral translation, respectively. As these motions are coupled, however, a two-degree-of-freedom normal-modes problem must be solved. The results are the natural frequencies, or eigenvalues, and mode shapes, or eigenvectors. The eigenvalue expressions are

$$\left(\frac{\varpi_1}{\varpi_r}\right)^2 = \frac{1}{2}\left[(\gamma\beta+1) - \sqrt{(\gamma\beta+1)^2 - 4\beta}\right] \tag{3}$$

$$\left(\frac{\varpi_2}{\varpi_l}\right)^2 = \frac{1}{2\beta}\left[(\gamma\beta+1) + \sqrt{(\gamma\beta+1)^2 - 4\beta}\right] \tag{4}$$

and the eigenvectors are given by

$$\left(\frac{\alpha h}{x}\right)_1 = 1 - \frac{1}{2\beta}\left\{(\gamma\beta+1) - \sqrt{(\gamma\beta+1)^2 - 4\beta}\right\} \tag{5}$$

$$\left(\frac{\alpha h}{x}\right)_2 = 1 - \frac{1}{2\beta}\left\{(\gamma\beta+1) + \sqrt{(\gamma\beta+1)^2 - 4\beta}\right\} \tag{6}$$

where

$$\gamma = \frac{J'}{J} \tag{7}$$

and

$$\beta = \left(\frac{\omega_l}{\omega_r}\right)^2. \tag{8}$$

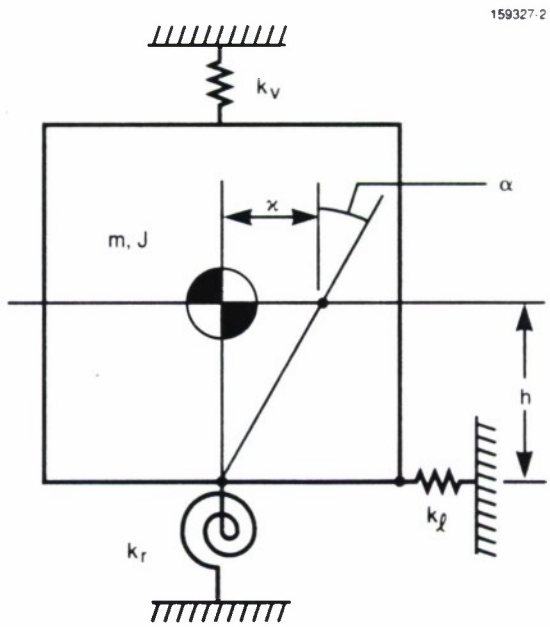

Figure 2. Simple planar rocking problem.

The eigenvalues [Equations (3) and (4)] give the location in the frequency domain of two **vibrational** modes, each sharing lateral and rocking motions [5]. The eigenvectors [Equations (5) and (6)] **ratio this** rocking to lateral motion to give a measure of the coupling of these two modes. The dimensionless parameters γ and ß are useful in studying the coupling between rotation and translation, in terms of the

uncoupled eigenvalues and mass distribution. Figures 3 and 4 show the effect on the eigenvalues and eigenvectors of varying γ and ß, respectively. Note that as γ approaches one, the second eigenvector approaches zero, and as ß gets large, the second eigenvector approaches zero.

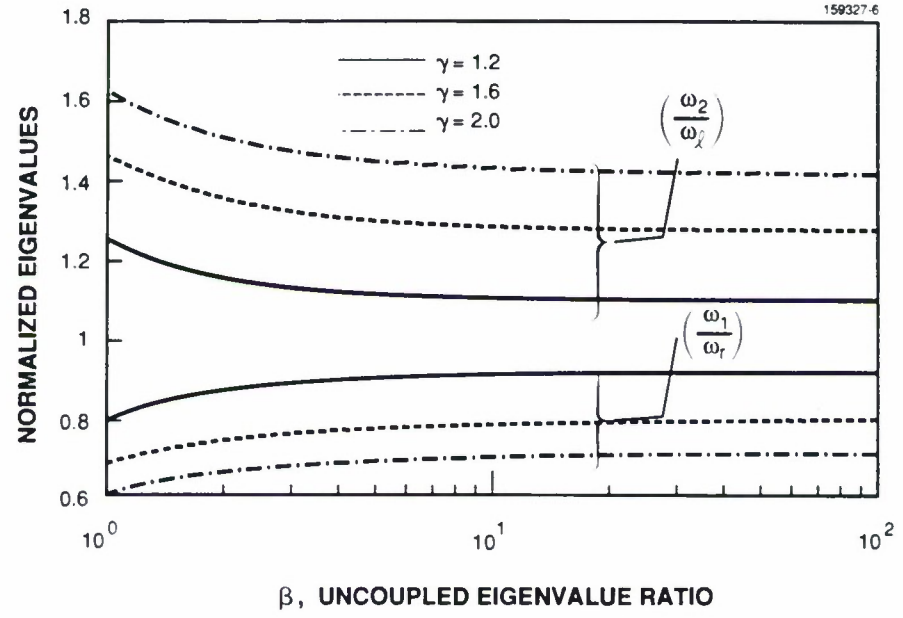

Figure 3. Normalized eigenvalues as a function of γ and ß. Note at γ close to one and ß large the coupled eigenvalues converge to their uncoupled counterparts.

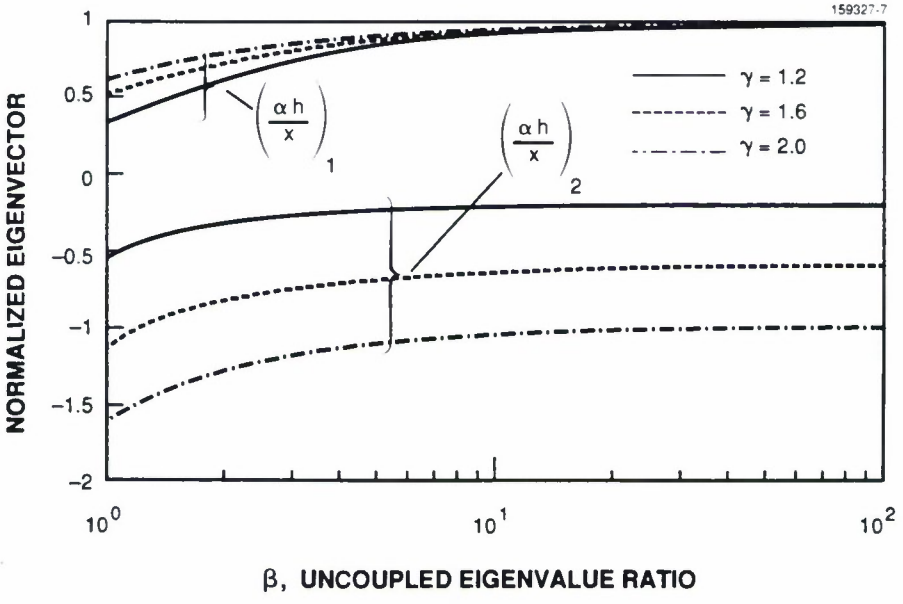

Figure 4. Eigenvectors as a function of γ and ß. Note at γ close to one and ß large the second eigenvector $(\alpha h/x)_2$ exhibits very little angle and predominantly translational motion in its mode shape. This behavior is desirable in the design of a stable high bandwidth control system.

This information is useful in determining the support flexure's geometry and stiffness based on the desired open-loop bandwidth, i.e., minimize coupling and place the second eigenvalue well away from the open-loop crossover.

Other contributors of these secondary modes are the mirror structure and housing. Finite-element analysis can verify that these possess high stiffness-to-weight ratios.

4. DESIGN OF THE HIGH-BANDWIDTH STEERING MIRROR

Figures 5 and 6 show the HBSM hardware resulting from the research program. Displayed are a mirror attached to four voice-coil actuators and to a flexural support held in a rigid housing. The support consists of an axial flexure and a flexure ring. The axial flexure reacts to motion along the mirror normal. The flexure ring constrains motions coplanar to the mirror surface and allows rotational compliance about an axes perpendicular to the mirror normal. The remaining degree of freedom, roll around the mirror normal, is resisted by the bipod geometry of the flexure ring. This arrangement allows a large value for β and a small value for γ, minimizing the second eigenvector's contribution to the mechanism frequency response. Stiffening the degrees-of-freedom attached to the mirror mass (those not being actuated) parallels an approach generated from the solution of the simple rocking problem. The γ may be interpreted as a coupling factor. In practice, this coupling is difficult to eliminate because of small asymmetries, mass, and actuation imbalances in the actual assembled steering mirror. For example, as witnessed in the laboratory, "piston" modes involving the mirror mass and axial flexure couple into the mirror tilting motions, and consequently into the servo loop. This effect is caused by the slight imbalance between opposing actuators, resulting in a torque and axial thrust at the mirror center of rotation. By driving ß, the square of the eigenvalue ratios, large, these coupling effects can be minimized. This is the underlying approach to the material selection and particular geometry making up the axial flexure and flexure ring parts.

Finally, a target plate, sandwiched between the actuator head and flexure ring, provides a conducting medium for the eddy current sensors. These sensors are used in the aforementioned acquisition loop.

A finite-element-based, steady-state frequency response analysis (MSC NASTRAN Version 65) was executed to verify that the system-transfer function between the linear force input by the actuators and the mirror tilt angle exhibited the desirable behavior indicated in Section 3. The NASTRAN results did show this response, approximated by a spring-mass-damper system with a natural frequency of 180 Hz and 5% critical damping. The mechanical roll-off (-40 dB/decade) following resonance showed negligible coupling up to 20 kHz. These results correlated well with the measured frequency response of the final unit.

Descriptions of the major individual piece parts follow.

4.1 MIRROR

The mirror was fabricated from one piece of beryllium with a Al/SiO surface coating. The surface figure was l/4p-v (632 nm wavelength) with a surface quality of 60/40, a reflectance of 90%, and a clear aperture of 16 mm. As this hardware was proof of concept, more stringent specifications on the mirror were not needed. (An alternative approach might epoxy a glass mirror or similar on a raised boss inside a counterbore to remove the mirror surface from the actuator load path.) The mirror's weight was reduced to obtain a higher stiffness-to-weight ratio. The mirror structure also transmits the push-pull linear forces into tilt motions. A trade-off exists in the mirror structure design: keeping the radius of gyration small, yet retaining a long lever arm to the actuator head. This trade-off was investigated and optimized.

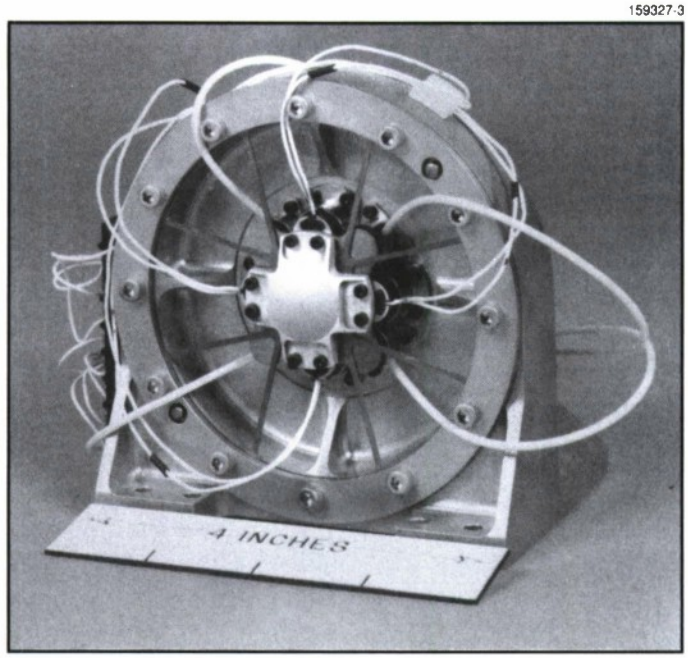

Figure 5. HBSM prototype hardware.

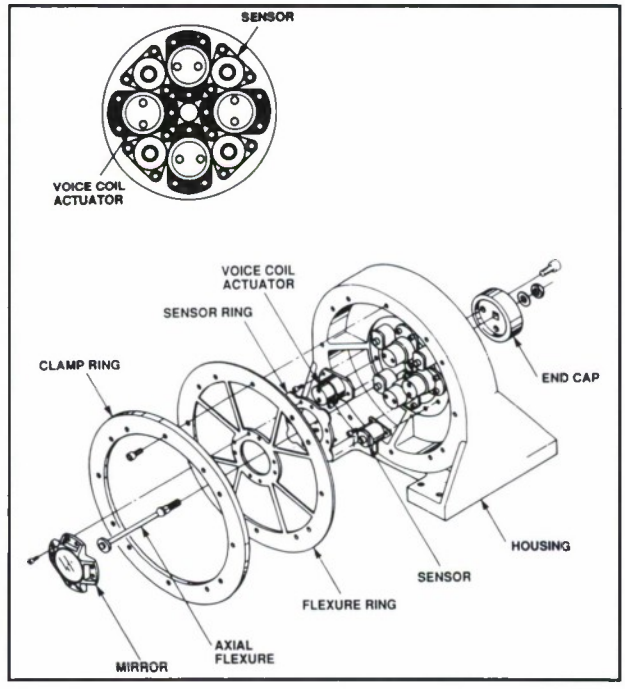

Figure 6. Exploded HBSM assembly. The particular flexure design yields g close to one and ß large. The second dominant eigenvector or mode does not couple into the mirror's actuated tilt motions. This scheme allows the system to function at higher bandwidth, yet retain good gain and phase margins.

4.2 FLEXURE

The axial flexure is a long, low section modulus reed offering little bending stiffness and high axial stiffness. This piece is machined out of aluminum alloy 7075-T6, which has high fatigue strength and low elastic modulus.

The flexure ring is made of stainless steel alloy 17-4 PH. Major concerns for this part arise from the need for good dimensional stability [6], high fatigue strength, machinability, and material uniformity. An electric discharge machine (EDM) was used to form the flexure ring, which has complex geometry and tight tolerances. The original blank was precipitation-hardened at 480°C before machining, and underwent a series of stabilizing heat treatments during manufacture.

To keep the part as symmetric as possible, the flexure ring was made from one piece. One of the drawbacks of this monolithic construction is that the main damping mechanism is the material's own internal friction. At frequencies over 1 kHz this value is very low, on the order of one-half of one percent critical damping [7]. Therefore, highly energetic bending resonances of the slender bipod legs appeared during open-loop testing. The solution was to apply a very thin layer of a viscoelastic material (3M 2216 Gray) to one side of the bipod legs to damp these bending modes. One important aspect in discussing effective damping materials is the loss factor, which is defined as the energy dissipated to the energy stored per cycle. Since the damping loss factor associated with viscoelastics is temperature and frequency dependent [8], a thorough analysis was done to choose an optimal material for the HBSM operating environment. An essentially constant loss factor was achieved over a broad temperature range (10 to 38°C) and frequency bandwidth. Installation of the damped flexure ring greatly improved the mechanism frequency response, with resulting negligible contribution of the aforementioned modes.

4.3 HOUSING

Since this research program was also concerned with building HBSMs that could eventually be flown on an airborne or space-based platform, reasonable weight and volume goals were chosen [0.7 kg and $(100\ \text{mm})^3$, respectively]. The housing design must provide a very stiff ground point to the actuators and flexural support. It is important that it not couple its own vibratory structural resonances to the mirror normal.

The prototype housing is machined from one aluminum alloy 6061-T6 billet. Its main features include gussetting to stiffen pitching motions and locating features to position the actuator and flexure assemblies accurately to a housing reference. The mass-loaded housing was finite-element modeled to verify adequate frequency response.

4.4 ACTUATORS

Four electromagnetic voice-coil actuators provide the beam steerer's motive power. These actuators were purchased from BEI Kimco (model number LA05A-05). The moving coil actuator consists of two parts, a coil bobbin and a permanent magnet and core assembly. The bobbin moves in an air gap through a permanent magnetic field when current flows through the coil. Current amplitude determines the magnitude of the force, and polarity the direction of actuation (push or pull). A rare earth magnet

(SmCo) is used as the permanent magnet to provide a high flux density in the air gap. When used with a restoring spring or flexure support, the actuation is linear and non-hysteretic, with good repeatability.

4.5 POSITION SENSORS

For the HBSM to accomplish its acquisition function, on-board position sensors are needed. This element, represented by the sensor block in Figure 1, actually senses position and transduces the measurement into a voltage. This signal is then fed to the HBSM controller. A two-channel Kaman KD-5100 differential measuring system was chosen. This sensor uses a small coil to emit a fluctuating magnetic field generating eddy currents in a conducting medium. The strength of the eddy current field is used to measure position. Some of the advantages of using the eddy-current sensor include high bandwidth, non-contacting, good sensitivity, and small volume.

This measuring device requires a target plate to furnish a conducting medium for the eddy currents. The manufacturer recommends that the target area be based on a minimum of twice the sensor diameter. The plate thickness is recommended to be at least triple the "skin depth" (a point below the surface of the target at which the eddy-current density drops to 36%). The target plate design is driven by the above, but again great effort was taken to ensure that no resonances below 20 kHz coupled into the servo loop. Because such a high stiffness-to-weight ratio was needed, the target plate was manufactured from beryllium. The target area was also minimized to keep its radius of gyration low.

To provide a tracking loop, the mirror was closed on a remote silicon photodiode quadrant detector. The quad cell and its ancillary electronics have high enough bandwidth to be considered a pure loop gain up to 20 kHz.

4.6 COMPENSATION/DRIVE ELECTRONICS

To complete the closed-loop system, a compensation network and current driver are added. The compensation network consists of a number of gain stages, two low-frequency integrators to increase the system's steady-state accuracy, and a lead network to boost the open-loop phase at crossover. The high bandwidth current drivers were custom-built at Lincoln Laboratory.

5. RESULTS AND DISCUSSION

As discussed, the HBSM prototype was implemented with two loops, track and acquisition. The track loop uses a HeNe laser, which is reflected off the center of the mirror and focused on the quadrant detector. The quad cell output is signal processed and fed to the HBSM controller (summing junction and compensation network). Rejection measurements were taken by inserting noise into the sensor output. Closed-loop rejection in the track mode is shown in Figure 7. Closed-loop response is shown in Figure 8, with a 10-kHz crossover at -3 dB. Because the compensation network was built with components on hand, some phase loss associated with the use of low-gain bandwidth product op-amps could easily be removed by implementing high-performance parts. This extra phase margin would help eliminate the +6 dB amplification at 6 kHz if this proved to be a problem.

Table 1 shows some of the resulting performance data for each loop configuration. The pointing accuracy in the track-loop configuration was measured by integrating the scaled-power spectral-density output from the quad cell over a frequency band of 1 Hz to 10 kHz. This value represents the mean square pointing error; root mean square error is given in the table. The data were taken in a laboratory environment.

Because the flexural support of the mirror is overconstrained, some concern was expressed for the nonlinear stiffness contributed by axial foreshortening in the bipod legs. This effect was not witnessed in test, due to the small actuator head displacement compared to the length of the bipod leg.

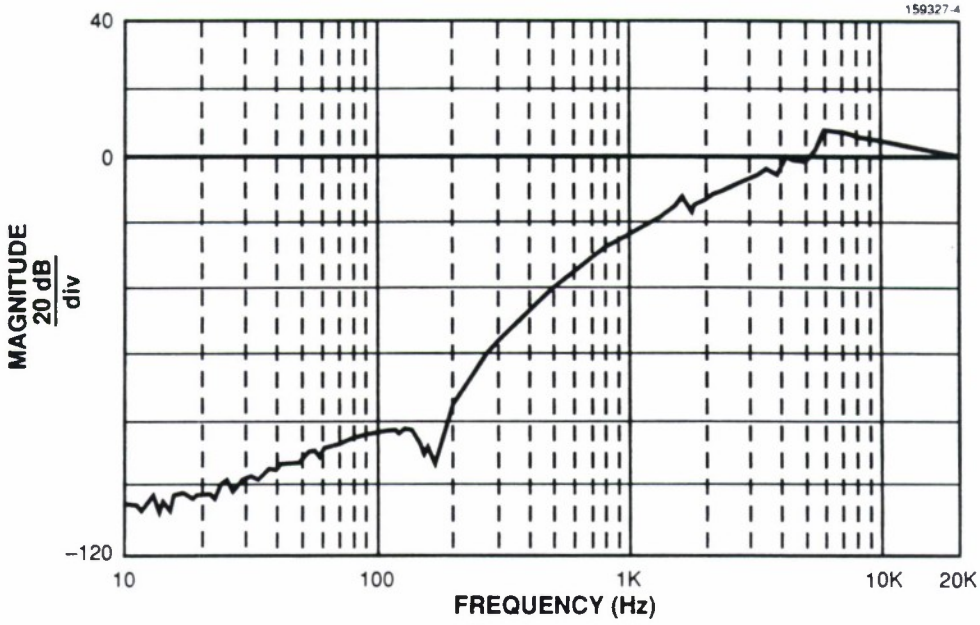

Figure 7. HBSM closed-loop rejection, elevation drive, track loop.

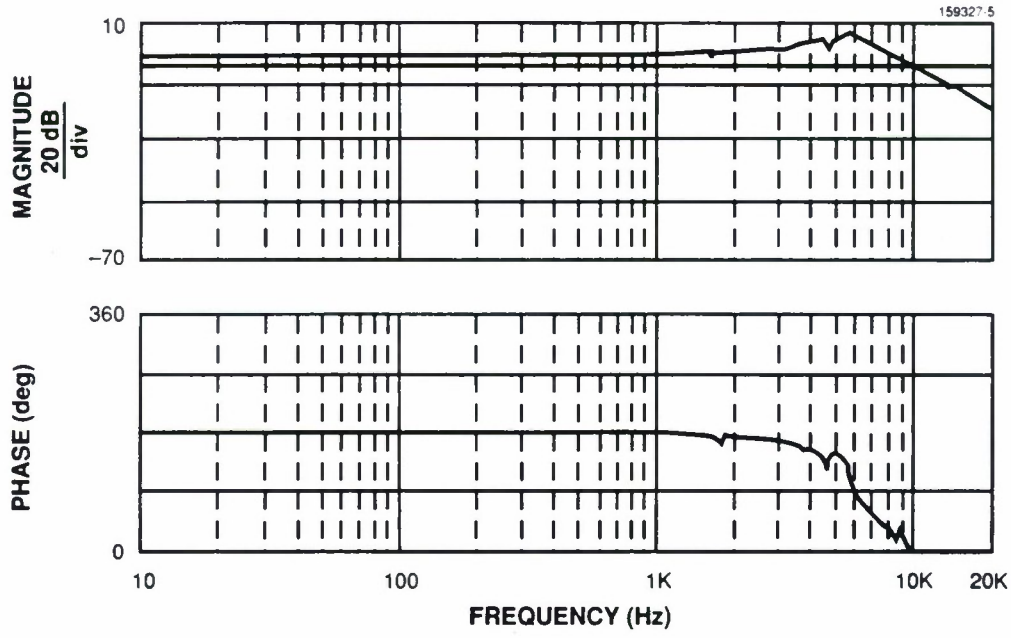

Figure 8. HBSM closed-loop response, elevation drive, track loop.

TABLE 1

HIGH BANDWIDTH STEERING MIRROR PROTOTYPE
Measured Performance

	VALUE	UNITS	COMMENTS
Aperture	16	mm	
Weight	0.7	kg	excluding electronics
Frontal Diameter	100	mm	
Power, typical	1	W	mechanism volume
Range	0.026	radian	peak-to-peak, shaft space
Closed-loop bandwidth			
Track	10	kHz	-3 dB crossing frequency
Acquisition	10		
Acceleration, peak	13	krad/s^2	
Phase margin	35	degrees	minimum value
Gain margin	6	dB	minimum value
Resolution	0.2	microradian	
Accuracy	0.2	microradian	rms error, track loop, laboratory environment
Repeatability	0.2	microradian	acquisition loop
Rejection			
100 Hz	-80	dB	tracking loop
500 Hz	-40		
1000 Hz	-20		
3000 Hz	-2		

6. SUMMARY

This investigation centered around an optimization of components common to small-aperture two-dimensional mechanical beam steerers. The design effort was directed at shaping a frequency response that allowed high-bandwidth closed-loop response with appropriate electronics. Simple rocking models were studied, and the results used to point out more advantageous flexure geometry. Numeric computational approaches were used to verify eventual system performance.

A thorough survey of materials useful to the HBSM technology was undertaken. These materials fall into two groups: those with high stiffness-to-weight properties, and those which are well damped and exhibit high strength (endurance limit). This damped feature may be achieved by passive techniques; in this case a viscoelastic material was coated on one side of the flexure ring. If the device must function over a certain temperature range, a careful analysis of the composite (metal/viscoelastic) part must be performed to assess the dependence of mechanical response on operating temperature.

The design approach started with a desired frequency response. Knowledge of materials technology, advances in manufacturing, and state-of-the-art analysis tools were used to achieve this response. The prototype hardware successfully met the research program goals, with 26-milliradian peak-to-peak stroke (mirror space) and a closed-loop bandwidth of 10 kHz. This performance indicates the benefits of closely scrutinizing the plant dynamics.

REFERENCES

1. Y. Netzer, "Line-of-sight steering and stabilization," *Opt. Eng.* 21(1), 096-104 (1982).
2. R. W. Cochran and R. H. Vassar, "Fast steering mirrors in optical control systems," in *Advances in Optical Structure Systems, Proc. SPIE 1303*, J. Breakwell, ed., (1990).
3. R.A. Lewis and L.R. Hedding, "Fast steering mirror design and performance for stabilization and single axis scanning," *Proc. SPIE 1304*, S. Gowrinathan, ed., (1990).
4. Y. Takahashi, M. J. Rabins, and D. M. Auslander, *Control and Dynamic Systems*, Reading, MA: Addison-Wesley Publishing Company, (1970).
5. W. T. Thomson, *Theory of Vibrations*, Englewood Cliffs, NJ: Prentice-Hall, Inc., (1972).
6. C. W. Marschall and R. E. Maringer, *Dimensional Instability*, Oxford: Pergamon Press, (1977).
7. C. Zener, *Elasticity and Anelasticity of Metals*, Chicago: University of Chicago Press, (1948).
8. A. D. Nashif, D. I. G. Jones, and J. P. Henderson, *Vibration Damping*, New York: John Wiley and Sons, (1985).

REPORT DOCUMENTATION PAGE

Form Approved
OMB No. 0704-0188

1. AGENCY USE ONLY *(Leave blank)*	2. REPORT DATE	3. REPORT TYPE AND DATES COVERED
	26 October 1990	Technical Report 1 Oct 88-30 Nov 89

4. TITLE AND SUBTITLE

Design of a Small-Aperture Steering Mirror for High-Bandwidth Acquisition and Tracking

5. FUNDING NUMBERS

C — F19628-90-C-0002

6. AUTHOR(S)

Gregory C. Loney

7. PERFORMING ORGANIZATION NAME(S) AND ADDRESS(ES)

Lincoln Laboratory, MIT
P.O. Box 73
Lexington, MA 02173-9108

8. PERFORMING ORGANIZATION REPORT NUMBER

Technical Report 903

9. SPONSORING/MONITORING AGENCY NAME(S) AND ADDRESS(ES)

Department of the Air Force

10. SPONSORING/MONITORING AGENCY REPORT NUMBER

ESD-TR-90-112

11. SUPPLEMENTARY NOTES

None

12a. DISTRIBUTION/AVAILABILITY STATEMENT

Approved for public release; distribution is unlimited.

12b. DISTRIBUTION CODE

13. ABSTRACT *(Maximum 200 words)*

The High-Bandwidth Steering Mirror (HBSM) prototype is the result of a research program to develop a beam steerer for optomechanical systems. The research centered on optimizing a beam-steering mechanism comprising a mirror, restoring flexure, actuators, position sensors, and encompassing housing. Design trade-offs and manufacturing issues are discussed and performance data presented.

14. SUBJECT TERMS

mirror
high bandwidth
beam compensation
pointing optics
fast-steering mirror

15. NUMBER OF PAGES
32

16. PRICE CODE

17. SECURITY CLASSIFICATION OF REPORT	18. SECURITY CLASSIFICATION OF THIS PAGE	19. SECURITY CLASSIFICATION OF ABSTRACT	20. LIMITATION OF ABSTRACT
Unclassified	Unclassified	Unclassified	SAR